Inorganic Chemistry

ARTICLE

pubs.acs.org/IC

Active-Site Models for the Nickel−Iron Hydrogenases: Effects of Ligands on Reactivity and Catalytic Properties

Maria E. Carroll, Bryan E. Barton, Danielle L. Gray, Amanda E. Mack, and Thomas B. Rauchfuss*

Department of Chemistry, University of Illinois at Urbana−Champaign, Urbana, Illinois 61801, United States

Supporting Information

ABSTRACT: Described are new derivatives of the type $[HNiFe(SR)_2(diphosphine)(CO)_3]^+$, which feature a Ni(diphosphine) group linked to a $Fe(CO)_3$ group by two bridging thiolate ligands. Previous work had described $[HNiFe(pdt)(dppe)(CO)_3]^+$ ($[\mathbf{1}H]^+$) and its activity as a catalyst for the reduction of protons (*J. Am. Chem. Soc.* **2010**, *132*, 14877). Work described in this paper focuses on the effects on properties of NiFe model complexes of the diphosphine attached to nickel as well as the dithiolate bridge, 1,3-propanedithiolate (pdt) vs 1,2-ethanedithiolate (edt). A new synthetic route to these Ni−Fe dithiolates is described, involving reaction of $Ni(SR)_2(diphosphine)$ with $FeI_2(CO)_4$ followed by in situ reduction with cobaltocene. Evidence is presented that this route proceeds via a metastable μ-iodo derivative. Attempted isolation of such species led to the crystallization of $NiFe(Me_2pdt)(dppe)I_2$, which features tetrahedral Fe(II) and square planar Ni(II) centers (H_2Me_2pdt = 2,2-dimethylpropanedithiol). The new tricarbonyls prepared in this work are $NiFe(pdt)(dcpe)(CO)_3$ (**2**, dcpe = 1,2-bis(dicyclohexylphosphino)ethane), $NiFe(edt)(dppe)(CO)_3$ (**3**), and $NiFe(edt)(dcpe)(CO)_3$ (**4**). Attempted preparation of a phenylthiolate-bridged complex via the $FeI_2(CO)_4$ + $Ni(SPh)_2(dppe)$ route gave the tetrametallic species $[(CO)_2Fe(SPh)_2Ni(CO)]_2(\mu\text{-}dppe)_2$. Crystallographic analysis of the edt-dcpe compund $[\mathbf{2}H]BF_4$ and the edt-dppe compound $[\mathbf{3}H]BF_4$ verified their close resemblance. Each features pseudo-octahedral Fe and square pyramidal Ni centers. Starting from $[\mathbf{3}H]BF_4$ we prepared the PPh_3 derivative $[HNiFe(edt)(dppe)(PPh_3)(CO)_2]BF_4$ ($[\mathbf{5}H]BF_4$), which was obtained as a ∼2:1 mixture of unsymmetrical and symmetrical isomers. Acid−base measurements indicate that changing from Ni(dppe) (dppe = $Ph_2PCH_2CH_2PPh_2$) to Ni(dcpe) decreases the acidity of the cationic hydride complexes by 2.5 pK_a^{PhCN} units, from ∼11 to ∼13.5 (previous work showed that substitution at Fe leads to more dramatic effects). The redox potentials are more strongly affected by the change from dppe to dcpe, for example the $[\mathbf{2}]^{0/+}$ couple occurs at $E_{1/2}$ = −820 for $[\mathbf{2}]^{0/+}$ vs −574 mV (vs $Fc^{+/0}$) for $[\mathbf{1}]^{0/+}$. Changes in the dithiolate do not affect the acidity or the reduction potentials of the hydrides. The acid-independent rate of reduction of CH_2ClCO_2H by $[\mathbf{2}H]^+$ is about 50 s^{-1} (25 °C), twice that of $[\mathbf{1}H]^+$. The edt-dppe complex $[\mathbf{2}H]^+$ proved to be the most active catalyst, with an acid-independent rate of 300 s^{-1}.

INTRODUCTION

Since the first crystallographic and IR spectroscopic evidence on their distinctive active sites,[1] the [NiFe]-hydrogenases have inspired many synthetic models.[2] Early work replicated the characteristic $Ni(SR)_2Fe$ subunit, and subsequent models incorporated CO and CN ligands bound to Fe.[3−5] Some early $Ni(SR)_2Fe$ compounds electrocatalyze the production of hydrogen from protons, although no intermediates have been established.[4,6] Recently, we described the first hydride-containing models that mimic *both* functional as well as certain structural features of the active sites of these enzymes (Figure 1).[7−9] Specifically, the hydride complex $[HNiFe(pdt)(dppe)(CO)_3]^+$ ($[\mathbf{1}H]^+$) was found to catalyze hydrogen evolution from acids at about −1.3 V vs $Fc^{+/0}$. The enzyme has also been shown to operate via hydride intermediates.[10] Although originally described as unstable,[11] **1** was found to be robust, reversibly protonated, and the resulting hydride is susceptible to substitution reactions.

With the goal of improving the catalytic properties of $[\mathbf{1}H]^+$, we have previously described changes in the iron subsite, leading to derivatives of the type $[HNiFe(edt)(dppe)(PR_3)(CO)_2]^+$, which also catalyze proton reduction.[9] In this report, we probe the influence of the dithiolate and the ligands on nickel. Unlike the active site of the [FeFe]-hydrogenase, the Ni and Fe centers in the [NiFe]-hydrogenases are linked by cysteinyl thiolates, but our previous models employed propanedithiolate (pdt), so variations of the thiolate were targeted. Furthermore, the terminal ligands on Ni in the protein are alkylthiolates, which are better donor ligands than arylphosphines.[12] To achieve the

Figure 1. Left: active site of the [NiFe]-hydrogenases in the SI-state, omitting possible protonation of terminal thiolate ligands. Right: functional models for the active site as discussed in this work.

Received: June 13, 2011
Published: August 25, 2011

Table 1. Selected IR Data (cm^{-1}, CH_2Cl_2 Solutions) for $NiFe(SR)_2(dxpe)(CO)_3$ and Derivatives

diphosphine, thiolate	$[(\mu\text{-I})NiFe(SR)_2(dxpe)(CO)_3]^+$	$NiFe(SR)_2(dxpe)(CO)_3$	$[HNiFe(SR)_2(dxpe)(CO)_3]^+$ (NMR $\delta_{hydride}$)
dppe, $S_2C_3H_6$	2096, 2054, 2023	2028, 1952	2082, 2024 (δ −3.53)
dppe, $S_2C_2H_4$	2095, 2046, 2028	2030, 1959	2084, 2025 (δ −5.7)
dppe, $(SPh)_2$	2082, 2032 (unstable)	2035, 1970 dimer[a]: 2001, 1942	
dcpe, $S_2C_3H_6$	2095, 2053, 2021	2014, 1940	2078, 2017 (δ −3.00)
dcpe, $S_2C_2H_4$	2096, 2075, 2053, 2029	2015, 1940	2080, 2019 (δ −5.3)

[a] "Dimer" refers to derivatives assumed to be $[(CO)_2Fe(SR)_2Ni(CO)]_2(\mu\text{-diphosphine})_2$. The monomeric NiFe complex was not observed for dppn. Similar results were obtained when starting with $Ni(SPh)_2(dcpe)$.

Scheme 1. Route to $NiFe(xdt)(dxpe)(CO)_3$ Complexes from $FeI_2(CO)_4$

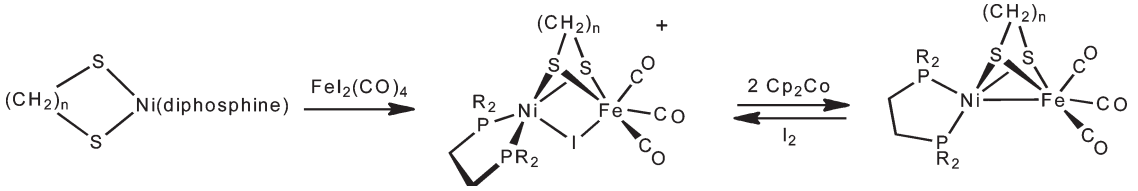

targeted changes in the ligands, we relied on the previously described[9] condensation of $Ni(SR)_2(diphosphine)$ with $Fe_2(CO)_9$, but we also developed a new route to such complexes that condenses ferrous carbonyls and $Ni(SR)_2(diphosphine)$ followed by reduction. We had reported a related reaction of $Fe(pdt)(CO)_2(dppe)$ with $NiCl_2(dppe)$ to afford salts of $[(\mu\text{-Cl})NiFe(pdt)(dppe)_2(CO)]^+$.[13] Until this work, we had not succeeded in converting such halide-bridged intermediates to the corresponding hydrides.

Setting aside the large volume of work on nickel-aminodiphosphine based catalysts[14] and those featuring $NiFeS_2$ cores discussed above, several Ni-containing bi- and polymetallic complexes have been shown to catalyze hydrogen evolution. One family of catalysts is based on Ru derivatives of NiN_2S_2 and NiS_4 metalloligands (N_2S_2 = diaminodithiolates and S_4 = dithioetherdithiolates).[15,16] Even oligomeric nickel dithiolates have been shown to catalyze proton reduction.[18] In other Ni−Fe complexes, catalysis was not observed when the Fe center is high spin.[17]

RESULTS AND DISCUSSION

Synthesis of $[NiFe(SR)_2(diphosphine)(CO)_3]^+$ Complexes. The condensation reaction of $Fe_2(CO)_9$ and $Ni(dithiolate)(diphosphine)$ provides a reliable route to complexes of the type $NiFe(dithiolate)(diphosphine)(CO)_3$ but cogenerates substantial amounts of $Fe_2(dithiolate)(CO)_6$. An alternative method that circumvents this side reaction was developed that employs $FeI_2(CO)_4$ as an Fe source. Thus, the reaction of $FeI_2(CO)_4$ and $Ni(pdt)(dppe)$ followed by addition of 2 equiv of Cp_2Co afforded **1** in ∼30% yield. Using the $Fe_2(CO)_9$ and the $FeI_2(CO)_4$ methods, we were able to generate complexes where pdt had been changed to edt and dppe was changed to dcpe (1,2-bis(dicyclohexylphosphino)ethane) (Table 1). Many additional building blocks were evaluated as described in the Supporting Information. For example, we initially attempted to prepare $Fe(CO)_3$ derivatives of $Ni(pdt)(dmpe)$, but these species were unstable, hence the use of the bulkier dcpe.

The $FeI_2(CO)_4$ method is proposed to proceed via the intermediacy of the μ-iodo cations $[(\mu\text{-I})NiFe(SR)_2(diphosphine)(CO)_3]^+$ (Scheme 1). IR spectra of these reaction solutions feature ν_{CO} bands resembling those for the corresponding hydride cations, but are shifted to higher energies by about 20 cm^{-1}. Spectra were somewhat more complicated than expected, probably owing to sample decomposition. Treatment of a CH_2Cl_2 solution of purified **1** with I_2 gave a simpler FT-IR spectrum (Figure 2).

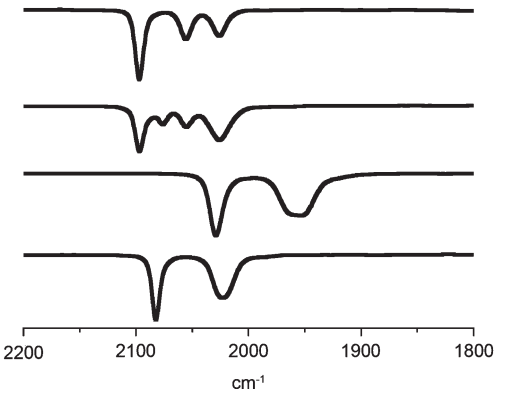

Figure 2. IR spectra (CH_2Cl_2 solutions, from top): $NiFe(pdt)(dppe)(CO)_3 + I_2$ (top), intermediate $[(\mu\text{-I})NiFe(pdt)(dppe)(CO)_3]I$ from the reaction of $Ni(pdt)(dppe) + FeI_2(CO)_4$, **1**, and $[\mathbf{1}H]BF_4$ (bottom).

In an effort to stabilize the μ-iodide intermediate, we investigated the reaction of $FeI_2(CO)_4$ with $Ni(Me_2pdt)(dppe)$, where Me_2pdt is 2,2,-dimethyl-1,3-propanedithiolate. This bulky dithiolate[19] was found to react with the iron reagent in the expected way as judged by IR spectra. The initial tricarbonyl product degraded, however, upon crystallization to the ferrous iodide derivative $NiFe(Me_2pdt)(dppe)I_2$, which was characterized by single crystal X-ray diffraction (Figure 3). As for other Ni(II)Fe(II) species, the Ni−Fe distance suggests the absence of metal−metal bonding. Related adducts of ferrous iodide with two thiourea ligands are known.[20] The formation of the ferrous iodide complex is proposed to occur via attack of the iodide counteranion at $[(\mu\text{-I})NiFe(pdt)(dppe)(CO)_3]^+$ concomitant with dissociation of the CO ligands.

dx.doi.org/10.1021/ic2012759 |Inorg. Chem. 2011, 50, 9554–9563

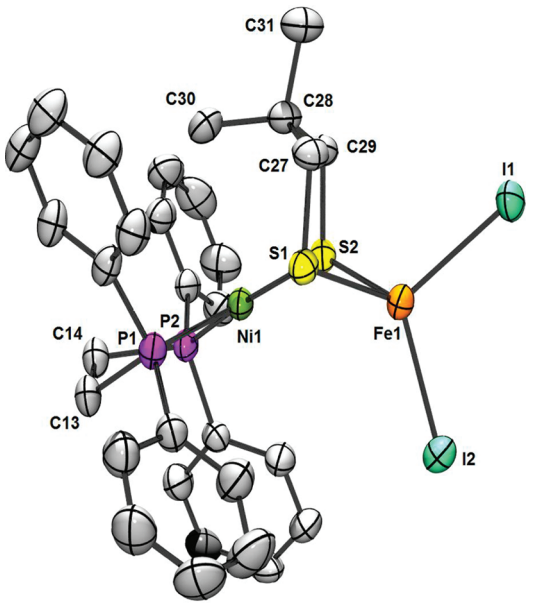

Figure 3. Structure of $NiFe(Me_2pdt)(dppe)I_2$. Selected distances (Å): Ni--Fe, 3.057; Ni1 P2 2.1703(12); Ni(1)−P(1), 2.1748(12); Ni(1)−S(2), 2.2296(12); Ni(1)−S(1), 2.2445(12); Fe(1)−S(2), 2.3806(12); Fe(1)−S(1), 2.3841(12); Fe(1)−I(2), 2.6165(7); Fe(1)−I(1), 2.6458(7).

Using the ferrous iodide method, we prepared three new NiFe complexes: $NiFe(pdt)(dcpe)(CO)_3$ (**2**), $NiFe(edt)(dppe)(CO)_3$ (**3**), and $NiFe(edt)(dcpe)(CO)_3$ (**4**), which are spectroscopically similar to $NiFe(pdt)(dppe)(CO)_3$.[11] Furthermore, all are stereochemically nonrigid as indicated by the observation of single resonances in the ^{31}P NMR spectra of each complex. Reminiscent of the observations on **1**,[9] the $^{31}P\{^1H\}$ NMR spectrum of **3** consists of a singlet at room temperature, but at lower temperatures the singlet decoalesces into two singlets (eq 1, Figure 4). For the analogous edt-dcpe complex **4**, the ^{31}P NMR signal remains a sharp singlet at −70 °C.

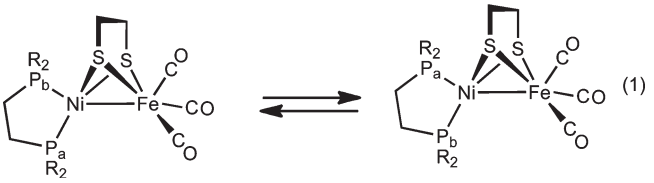

SPh Derivatives. We attempted to prepare $NiFe(SR)_2$ compounds using the bis(monothiolate) complex $Ni(SPh)_2(dppe)$. We expected that the unidentate thiolate would more accurately mimic the μ-cysteinate ligands in the active site of the [NiFe]-hydrogenases. $Ni(SPh)_2(dppe)$ was indeed found to react with $FeI_2(CO)_4$, and the product of this reaction underwent reduction by Cp_2Co. The same product was obtained from the reaction of $Ni(SPh)_2(dppe)$ and $Fe_2(CO)_9$. Crystallographic analysis indicated that this derivative is $[(CO)_2Fe(SPh)_2Ni(CO)]_2(\mu\text{-dppe})_2$ (eq 2, Figure 5). The crystallographic result is corroborated by the ^{31}P NMR spectrum. This spectrum features doublets of doublets at δ 33.9 and at 49.9 (J_{PP} = 30, 60 Hz), which are consistent with symmetrically oriented SPh ligands. The FT-IR spectrum (ν_{CO} = 1993, 1938 cm^{-1}) resembles that reported for $(CO)_2Fe(pdt)Ni(CO)(\mu\text{-dppe})$.[11] The reaction of $Ni(SPh)_2(dppbz)$ appeared to give a similar a product (ν_{CO} = 2006(s), 1945(m) cm^{-1}). In view of the successes described above with Ni(pdt)(dcpe), we examined the reaction $Ni(SPh)_2(dcpe)$ + $FeI_2(CO)_4$. Reduction of the iodo intermediate with Cp_2Co gave $NiFe(SPh)_2(dcpe)(CO)_3$ complex as indicated in the IR spectrum; however, this initial product isomerized rapidly to a species spectroscopically analogous to $[(CO)_2Fe(SPh)_2Ni(CO)]_2(\mu\text{-dppe})_2$.

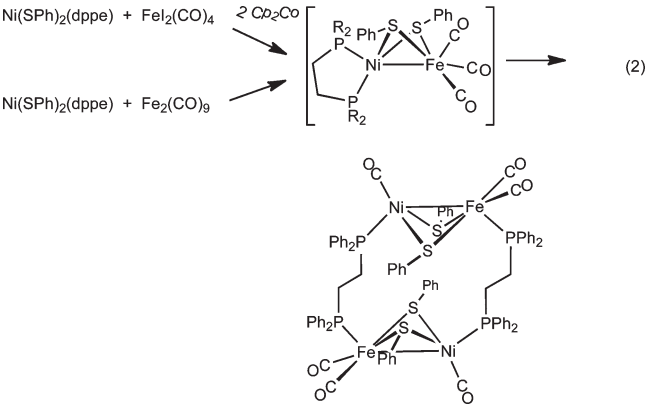

Redox Properties of 2, 3, and 4. As previously reported, **1** oxidizes reversibly at −0.57 V vs $Fc^{0/+}$ in benzonitrile solution with $[NBu_4]PF_6$ as electrolyte.[9] As a solvent for the neutral complexes, PhCN is superior to MeCN, but the redox potentials are assumed to be the same, that is, $E^{PhCN} = E^{MeCN}$.[21] Complex **2** oxidizes reversibly at −0.82 V vs $Fc^{0/+}$, 250 mV milder than the $[\mathbf{1}]^{0/+}$ couple. Similarly, the dcpe-edt complex **4** oxidizes at −0.74 V, 300 mV milder than the $[\mathbf{3}]^{0/+}$ couple. Thus, the basicity of the diphosphine significantly affects the redox potentials, but the identity of the dithiolate bridge has little effect. For **1**, **2**, **3** and **4**, a second irreversible oxidation is observed at more positive potentials than the first oxidation (Table 2). We assign all couples to one-electron events, as was verified for **1**.[9]

Characterization of New Tricarbonyl Hydrides. Protonation of the reduced species, **2**, **3**, and **4**, with $HBF_4 \cdot Et_2O$ gave the corresponding hydrides, the new salts being $[HNiFe(pdt)(dcpe)(CO)_3]BF_4$ ($[\mathbf{2H}]BF_4$), $[HNiFe(edt)(dppe)(CO)_3]BF_4$ ($[\mathbf{3H}]BF_4$), and $[HNiFe(edt)(dcpe)(CO)_3]BF_4$ ($[\mathbf{4H}]BF_4$). These complexes were also characterized by $^{31}P\{^1H\}$ and ^1H NMR spectroscopy. Illustrative of the stability of these complexes, the NMR spectrum of a CD_2Cl_2 solution of the edt-dppe cation $[\mathbf{3H}]^+$ was found to remain unchanged in the presence of 500 equiv of trifluoroacetic acid after 5 h at room temperature.

Salts $[\mathbf{2H}]^+$ and $[\mathbf{3H}]^+$ were further characterized by single crystal X-ray diffraction (Figures 6, 7, Table 3). Overall, the NiFe cations closely resemble $[\mathbf{1H}]^+$.[7] In the crystallographic analyses, the hydride ligands were located and refined. The Ni−H−Fe linkage is unsymmetrical in all cases, with the Fe−H distance shorter than the Ni−H distance by 0.18 and 0.37 Å for $[\mathbf{2H}]BF_4$ and $[\mathbf{3H}]BF_4$, respectively. At 2.68 Å, the Ni−Fe distance is elongated in the bulkier dcpe complex $[\mathbf{2H}]^+$ vs 2.61 and 2.60 Å in $[\mathbf{1H}]^+$ and $[\mathbf{3H}]^+$, respectively.[7]

$[HNiFe(edt)(dppe)(PPh_3)(CO)_2]BF_4$. The substituted edt derivative $[HNiFe(edt)(dppe)(PPh_3)(CO)_2]BF_4$ ($[\mathbf{5H}]BF_4$) was prepared by substitution of one CO in $[\mathbf{3H}]BF_4$ with PPh_3. Interestingly, NMR spectra indicate the presence of two isomers in a ratio of ~2:1. Each isomer exhibits a doublet-of-triplets in the hydride region of the ^1H NMR spectrum. For $[HNiFe(pdt)(dppe)(PPh_3)(CO)_2]BF_4$, we had previously detected trace amounts

dx.doi.org/10.1021/ic2012759 |Inorg. Chem. 2011, 50, 9554–9563

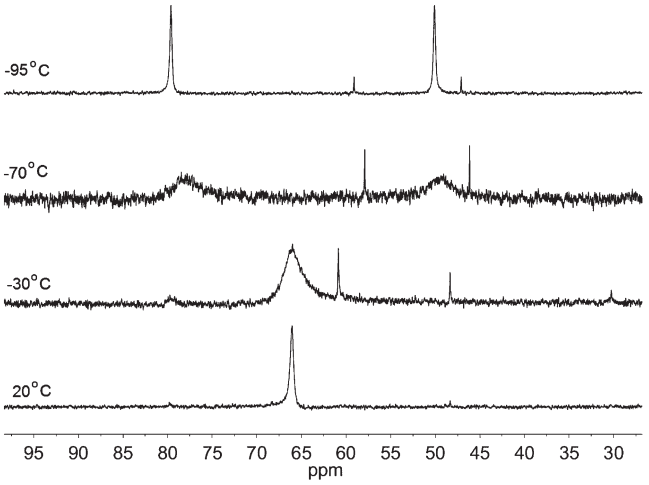

Figure 4. $^{31}P\{^{1}H\}$ NMR spectra of **3** (500 MHz, THF-d_8 solution) at various temperatures. The signal at ~δ60 corresponds to Ni(edt)(dppe), and the signal at ~δ47 is unassigned.

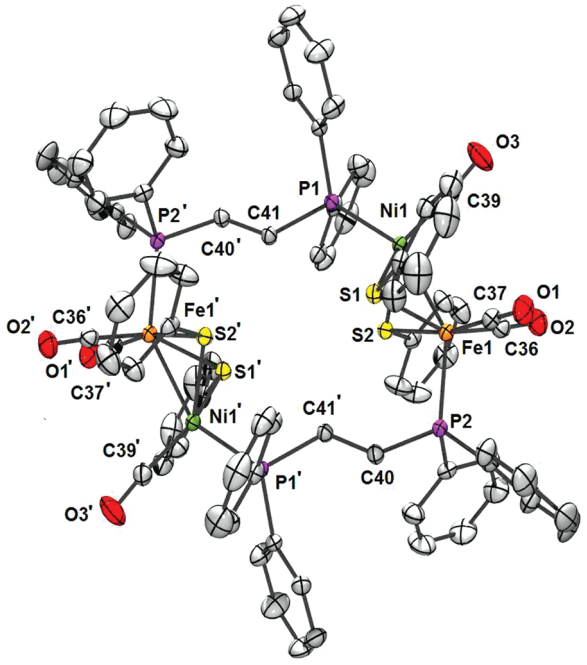

Figure 5. Structure of $[(CO)_2Fe(SPh)_2Ni(CO)]_2(\mu$-dppe$)_2$. Selected distances (Å): Ni—Fe, 2.4567(3); Fe(1)—P(2), 2.2326(5); Ni(1)—P(1), 2.1905(5); Ni(1)—S(1), 2.2633(5); Ni(1)—S(2), 2.2784(5); Fe(1)—S(1), 2.2833 (5); Fe(1)—S(2) 2.3167(6).

of a second isomer, but the mole fraction was so small that the nature of this minor component was unclear.[9] By comparisons of the ^{1}H NMR shifts with those for the pdt derivatives, the major isomer in $[\mathbf{5H}]BF_4$ is unsymmetrical (as is the predominant isomer of $[HNiFe(pdt)(dppe)(PPh_3)(CO)_2]^+$),[9] with the PPh_3 ligand in a basal position (Scheme 2). The occurrence of about 30% of an isomer with PPh_3 in the apical position apparently reflects the moderate steric profile of edt vs pdt.

The sym- and unsym-isomers of $[\mathbf{5H}]^+$ do not readily interconvert although variable temperature $^{31}P\{^{1}H\}$ spectra indicate

Table 2. Selected Electrochemical Properties (V vs $Fc^{+/0}$) of $Fe^{I}Ni^{I}$ Complexes[a]

compound	$E_{1/2}$, $NiFe^{0/+}$	i_{pa}/i_{pc}	E_{pa}[b], $NiFe^{+/2+}$
NiFe(pdt)(dppe)$(CO)_3$, **1**	−0.580	0.93	−0.036
NiFe(pdt)(dcpe)$(CO)_3$, **2**	−0.820	0.95	+0.220
NiFe(edt)(dppe)$(CO)_3$, **3**	−0.540	0.33	−0.075
NiFe(edt)(dcpe)$(CO)_3$, **4**	−0.740	0.80	+0.027

[a] Conditions: scan rate 100 mV/s, benzonitrile solution. [b] E_{pa} = peak potential for cathodic peak for second oxidation, this couple being irreversible.

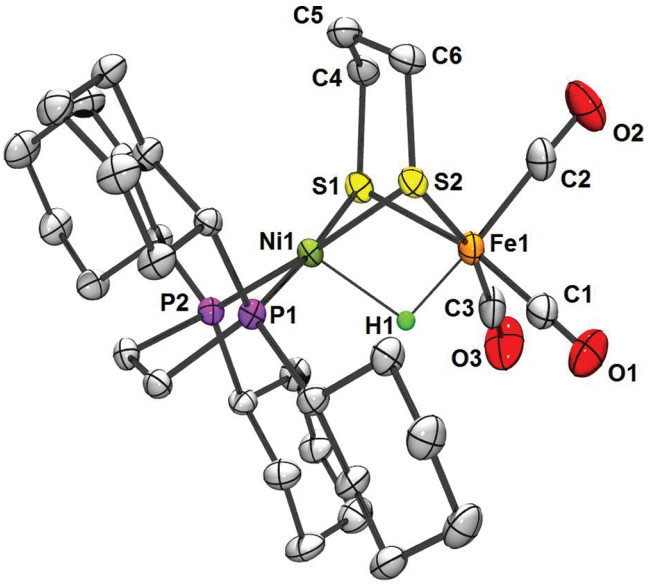

Figure 6. Molecular structure of the cation $[\mathbf{2H}]^+$ in $[HNiFe(pdt)(dcpe)(CO)_3]BF_4$. Hydrogen (except the hydride ligand) atoms and BF_4^- are not shown. Selected distances (Å): Ni—Fe, 2.6843(5); Ni—S(1), 2.2274(7); Ni—S(2), 2.2307(7); Fe—S(1), 2.3208(8); Fe—S(2), 2.3169(8); Ni—H, 1.90(2); Fe—H, 1.53(2).

that the unsym isomer is dynamic on the NMR time scale such that only one signal is observed for the dppe ligand in each isomer (Figure 8). When a CD_2Cl_2 solution of $[\mathbf{5H}]^+$ is cooled, the signal assigned to the dppe on the unsym isomer broadens. Although not examined explicitly, it is likely that dppe in the symmetric isomer is also nonrigid (Scheme 2). These observations underscore the stereochemical flexibility of the square pyramidal nickel sites in these hydrido complexes. Deprotonation of $[\mathbf{5H}]^+$ with Et_3N gave the neutral complex **5**, which was characterized by IR and ^{1}H and ^{31}P NMR spectroscopy.

Redox Properties of $[\mathbf{2H}]^+$, $[\mathbf{3H}]^+$, $[\mathbf{4H}]^+$, and $[\mathbf{5H}]^+$. The reduction of the hydrides was also examined. For the couple $[\mathbf{1H}]^{+/0}$, E^{MeCN} is −1.29V vs $Fc^{0/+}$. The $[\mathbf{1H}]^{+/0}$ couple is partially reversible, whereas little reversibility was detected in the couples $[\mathbf{2H}]^{+/0}$, $[\mathbf{3H}]^{+/0}$, $[\mathbf{4H}]^{+/0}$, and $[\mathbf{5H}]^{+/0}$ (Table 3). Changing the solvent to CH_2Cl_2 did not substantially improve the reversibility of any of the hydrides. In the case of $[\mathbf{1H}]^{+/0}$, varying the scan rate from 100 to 750 mV/s improved the reversibility from i_{pa}/i_{pc} from 0.26 to 0.8. The irreversibility of

dx.doi.org/10.1021/ic2012759 |Inorg. Chem. 2011, 50, 9554–9563

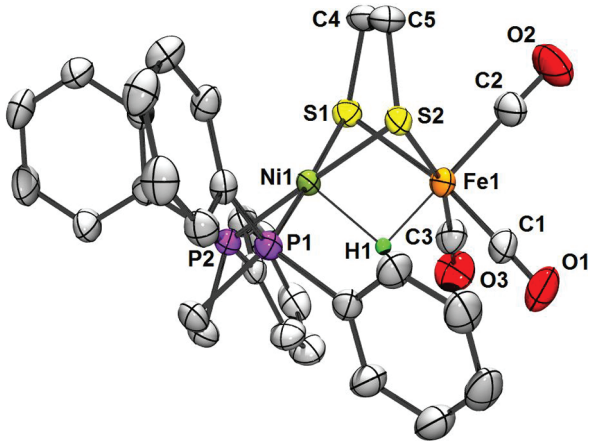

Figure 7. Molecular structure of the cation in [[HNiFe(edt)-(dppe)(CO)$_3$]$^+$ ([**4H**]$^+$). Hydrogen (except the hydride ligand) atoms and BF_4^- are not shown. Selected distances (Å): Ni—Fe, 2.5958(6); Ni—S(1), 2.1969(9); Ni—S(2), 2.2128(9); Fe—S(1), 2.3152(9); Fe—S(2), 2.328(1); Ni—H, 1.84(3); Fe—H, 1.58(4).

Table 3. Selected Bond Distances (Å) for [HNiFe(xdt)(dxpe)(CO)$_3$]BF$_4$

	Ni—Fe	Ni—H	Fe—H	Δ(Ni—H, Fe—H)
[**1H**]BF$_4$	2.61	1.64	1.46	0.18
[**2H**]BF$_4$	2.68	1.91	1.53	0.38
[**3H**]BF$_4$	2.59	1.84	1.58	0.26

the [**1H**]$^{+/0}$ couple is due to an intermolecular conversion of [**1H**]^0 into **1**, as indicated by the appearance of a reversible couple at −0.58 V corresponding to [**1**]$^{+/0}$ (Table 2). Similarly, events for the [**2**]$^{+/0}$ couple appear upon repeated redox cycles for the [**2H**]$^{+/0}$ couple. Compared to E^{MeCN} for [**1H**]$^{+/0}$ at −1.29 V, [**2H**]$^+$ reduces at −1.49 V (Table 4). Thus, the basicity of the Ni center more modestly affects the [**1H**]$^{+/0}$ couple than the [**1**]$^{+/0}$ couple.

Electrocatalysis. These experiments employed CH_2Cl_2 solutions of the hydride salts; MeCN solutions are stable only for a few minutes at room temperature. As can be seen in Table 4, the reduction potentials for CH_2Cl_2 and MeCN solutions are similar. For each hydride complex, the i_{pc} was found to increase with the addition of the acid indicating catalytic reduction of protons. For the less basic dppe derivatives, we used trifluoroacetic acid (pK_a^{MeCN} = 12.65),[22] whereas for the more basic catalysts, the weaker chloroacetic acid (pK_a^{MeCN} = 15.3) was used. So long as the pK_a of the acid is below that of the NiFe hydride catalyst, the nature of the acid has little influence on rates in the plateau region.

Some insight into the catalytic mechanism is provided by the effect of [H$^+$] on i_c/i_p, where i_c is the catalytic current and i_p is the peak current for reduction of the hydride complex in the absence of additional acid. For small values of [H$^+$], i_c increases linearly, consistent with the dependence of the rate of hydrogen evolution on protonation of the reduced hydride.[21] The relative catalytic activity (k) of the Ni—Fe hydrides was estimated by the value of i_c/i_p

Scheme 2. Dynamic Equilibria Proposed for Isomers of [HNiFe(edt)(dppe)(PPh$_3$)(CO)$_2$]$^+$

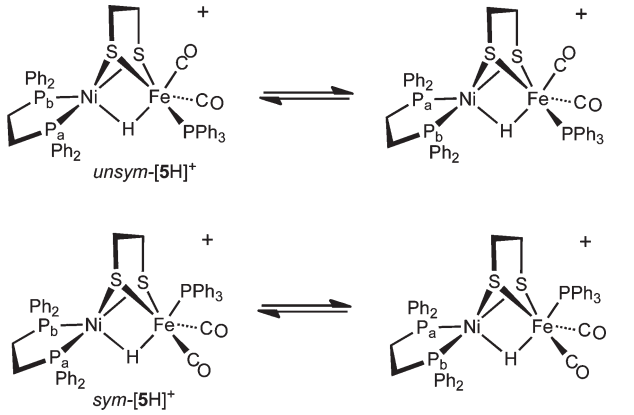

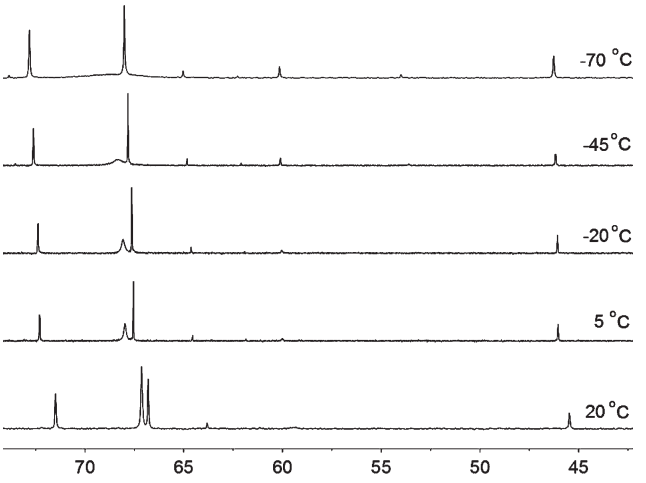

Figure 8. Variable temperature $^{31}P\{^1H\}$ NMR (202 MHz, CD_2Cl_2) spectra of [HNiFe(edt)(dppe)(PPh$_3$)(CO)$_2$]BF$_4$. The signal at δ 68, assigned to the phosphorus centers of dppe on the unsymmetrical isomer, broadens at −70 °C, indicative of slowed rotation of the dppe ligand at the Ni center. The signal at δ 45 is assigned to PPh$_3$ on the symmetrical isomer. Signals at δ 72 and 66 correspond to PPh$_3$ on the unsymmetrical isomer and dppe on the symmetrical isomer, but further assignments cannot be made, based on this data.

in the regime where the catalytic rate is independent of

$$i_c/i_p = (n/0.446)(RTk/Fv)^{1/2} \quad (3)$$

[H$^+$] (eq 3).[21] For [**2H**]$^+$, the observed value of $[i_c/i_p]_{max}$ of ∼15 corresponds to an acid-independent turnover frequency of ∼50 s^{-1}, about twice the rate of the related dppe derivative.[9]

Like the propanedithiolate [**1H**]$^+$, the ethanedithiolate [**3H**]$^+$ catalyzes hydrogen evolution from CF_3CO_2H. E_{cat} for [**1H**]$^+$ and [**3H**]$^+$ differ by only 140 mV, but [**3H**]$^+$ is far more active (Figure 9, 10). Specifically, the observed $[i_c/i_p]_{max}$ of 35−40 indicates a turnover frequency of 240−310 s^{-1}. This rate is about 10× that of [**1H**]$^+$ and is comparable to some nickel-diaminodiphosphine catalysts.[24] When the catalyst concentration was halved (0.25 mM vs 0.5 mM), the rate in the

dx.doi.org/10.1021/ic2012759 |Inorg. Chem. 2011, 50, 9554–9563

Table 4. Selected Electrochemical Properties (V vs $Fc^{+/0}$) of $[HNiFe(xdt)(dxpe)(CO)_3]BF_4$ in CH_2Cl_2[a]

complex	$E([HNiFe]^{+/0})$ (MeCN)	i_{pa}/i_{pc} (MeCN)	$E([HNiFe]^{+/0})$ (CH_2Cl_2)	i_{pa}/i_{pc} (CH_2Cl_2)
$[HNiFe(pdt)(dppe)(CO)_3]BF_4$, $[1H]BF_4$	−1.29	0.26	−1.34	0.26
$[HNiFe(pdt(dcpe)(CO)_3]BF_4$, $[2H]BF_4$	−1.49	0.11	−1.56	0.10
$[HNiFe(edt)(dppe)(CO)_3]BF_4$, $[3H]BF_4$	−1.33	0	−1.33	0.08
$[HFeNi(edt)(dcpe)(CO)_3]BF_4$, $[4H]BF_4$	−1.41	0	−1.47	0
$[HNiFe(edt)(dppe)(PPh_3)(CO)_2]BF_4$, $[5H]BF_4$	−1.54	0	−1.47	0

[a] Conditions: 0.5 M catalyst, scan rate 100 mV/s.

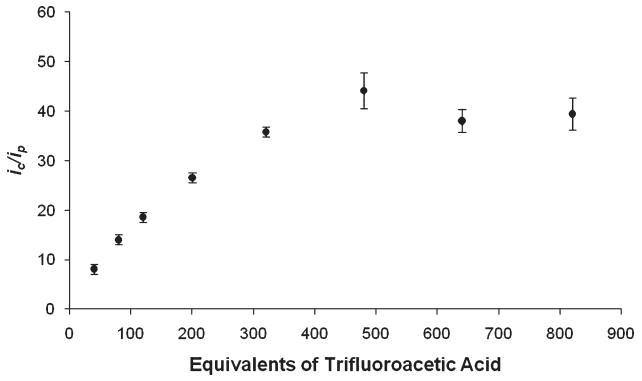

Figure 9. Dependence of normalized catalytic current i_c (1.3 V vs $Fc^{+/0}$) for 0.5 mM $[3H]^+$ on $[CF_3CO_2H]$. The graph shows data for three experiments.

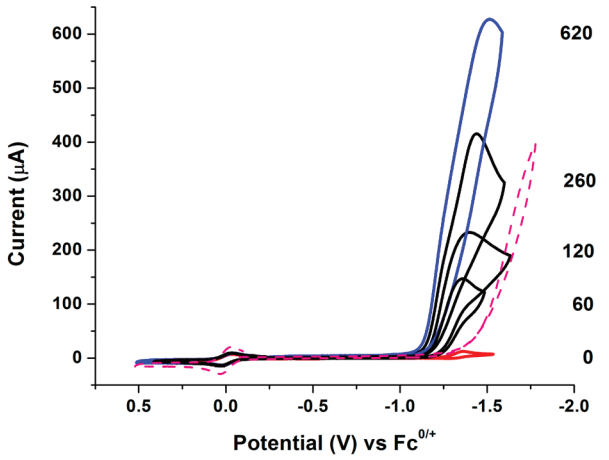

Figure 10. Cyclic voltammogram of $[3H]^+$ before (solid red line) and after addition of varying equiv (denoted on right) of CF_3CO_2H. A voltammogram in the absence of $[3H]^+$ at 620 equiv of acid is shown with dotted red line. Conditions: ~0.5 mM $[3H]^+$ in CH_2Cl_2, 0.1 M $[NBu_4]PF_6$, scan rate 0.1 V/s, glassy carbon working electrode (d = 3.0 mm); Ag wire pseudoreference with internal Fc ($E_{1/2} \equiv 0$ V); Pt counter electrode.

acid-independent regime remained unchanged, verifying that the rate is independent of catalyst concentration.

We previously reported that substitution of CO with PPh_3 in $[1H]^+$ resulted in a 2-fold increase in the rate of catalysis. When the analogous substitution is made with the ethanedithiolate $[3H]^+$, increasing amounts of CH_2ClCO_2H cause an increase in the reductive current at −1.5 V. Graphs of i_c/i_p vs acid concentration begin to plateau at ~500 equiv of acid, corresponding to i_c/i_p of 25. However, the value of i_c/i_p decreases with additional acid, an effect we tentatively attribute to catalyst decomposition (See Supporting Information). On the basis of these results, $[5H]^+$ operates at a slower rate than the analogous tricarbonyl derivative $[3H]^+$. Note, however, that $[5H]^+$ exists as a mixture of two isomers, in a ratio of ~2:1, and one of the two isomers is likely a more active catalyst.

Overpotential. The overpotential of these catalysts for hydrogen evolution is determined by the pK_a's and reduction potentials of the hydrides $[HNiFe]^{+/0}$. Both the relevant pK_a's and redox potentials were determined in MeCN (or PhCN) solutions, where overpotential can be meaningfully calculated,[23] although catalysis was conducted in CH_2Cl_2 because the catalysts are more stable in this solvent. Our measurements indicate that $(E^{CH_2Cl_2} - E^{MeCN})$ is ≤70 mV (Table 4). Acid−base titrations were conducted on PhCN solutions of the hydrides, since the neutral conjugate bases are poorly soluble in MeCN. Using aniline (pK_a^{MeCN} = 10.7), the pK_a^{PhCN} of $[1H]^+$ was shown by ^{31}P NMR spectroscopy to be 10.8 vs 10.7 previously determined by IR spectroscopy.[9] The pK_a^{PhCN} for the related edt complex $[3H]^+$ is 11.3. In the case of the edt-dcpe complex $[4H]^+$, the pK_a^{PhCN} was determined to be 13.6 using 4-methoxypyridine (pK_a^{MeCN} 14.23).[25] Deprotonation of the pdt-dcpe hydride was too slow to allow precise determination of the pK_a; we note, however, that the pK_a's of the edt-dcpe and pdt-dcpe hydrides were similar.

Theoretical potentials for the reduction of these hydrides were estimated from E^{MeCN} and pK_a^{PhCN}. Adapting the approach of Evans and Artero et al.,[23] the potential for catalytic proton reduction, E_{cat}, was assigned to the potential corresponding to half the catalytic current in the acid-independent regime. This value was approximately 100 mV positive of $E([HNiFe]^{+/0})$. We estimate that the errors for the overpotentials in Table 5 are ±50 mV.

CONCLUSION

The [NiFe]-hydrogenases operate via intermediates with a (μ-H)NiFe(SR)$_2$ core, and this paper contributes new examples of such bioinspired catalytic intermediates.[9] In this report, we explored the effect of coligands (on nickel) and the dithiolate on the catalytic and other chemical properties of dithiolato NiFe hydrides.

A promising new entry to these complexes proceeds via the reaction of nickel dithiolates with $FeI_2(CO)_4$. This ferrous carbonyl iodide and the related bromide have been widely used for the preparation of ferrous carbonyls.[26,27] Typical substitution reactions of $FeI_2(CO)_4$ replace one or more CO ligands with $2e^-$ donors to give complexes of the type $FeI_2L_2(CO)_2$ or $[FeX_3(CO)_3]^-$.[27] The

dx.doi.org/10.1021/ic2012759 |Inorg. Chem. 2011, 50, 9554–9563

Table 5. Parameters for Hydrogen Evolution Catalyzed by NiFe Hydrides in CH_2Cl_2 Solution (Potentials in V vs $Fc^{0/+}$)

hydride catalyst, proton source	E_{cat} [a]	overpotential[b]	rate,[c] s^{-1}	pK_a of hydride[d]
$[HNiFe(pdt)(dppe)(CO)_3]^+$ ($[\mathbf{1}H]^+$), CF_3CO_2H	−1.20	0.50	20	10.7
$[HNiFe(pdt)(dcpe)(CO)_3]^+$ ($[\mathbf{2}H]^+$), CH_2ClCO_2H	−1.46	0.59	50	∼13.6
$[HNiFe(edt)(dppe)(CO)_3]^+$ ($[\mathbf{3}H]^+$), CF_3CO_2H	−1.23	0.49	240−310	11.3
$[HNiFe(edt)(dcpe)(CO)_3]^+$ ($[\mathbf{4}H]^+$), CH_2ClCO_2H	−1.45	0.59	20	13.6
$[HNiFe(edt)Ni(dppe)(PPh_3)(CO)_2]BF_4$ ($[\mathbf{5}H]^+$), CH_2ClCO_2H	−1.45	0.54	60−120	14.0

[a] E_{cat} is the potential at half-height in the $[H^+]$-independent regime (CH_2Cl_2 solutions).[23] [b] Overpotentials calculated from $|E_{cat} - E(H_2/HA)|$. For MeCN solutions, $E(H_2/H^+) = -0.07$ V and $E(H_2/HA)$ is more negative, depending on the pK_a of HA (see Supporting Information).[23] [c] Rate at $[H^+]$-independent regime (see Figure 9). [d] In PhCN solutions, determined using pyridine/pyridinium derivatives as base/acid (see text).

intermediate $[(\mu\text{-I})NiFe(SR)_2(diphosphine)(CO)_3]^+$ is structurally analogous to the hydrido cations. We had characterized $[(\mu\text{-Cl})NiFe(pdt)(dppe)_2(CO)]^+$.[7,13] Both the μ-hydride and the μ-iodo tricarbonyls reduce readily to give the targeted Ni(I)Fe(I) derivatives. It is curious that the μ-iodo complexes are more labile than the corresponding μ-hydrido cations. We ascribe this difference to the stabilizing influence of the strong σ-donor hydride which stabilizes CO ligands on these midvalent complexes.[28]

It is instructive to compare these $[HNiFe(xdt)(CO)_{3-x}(PR_3)_x(diphosphine)]^+$ catalysts and other NiFe-based catalysts. Complexes of the present type are simpler to analyze since the hydride complexes are directly observable. In contrast, for other Ni−Fe systems, the catalysts are generated in situ and hydride intermediates are not observed spectroscopically.[6,15,18,29] Because the pK_a's of our hydrides can be determined, overpotentials can be determined with useful precision. Most active site models for the NiFe-hydrogenases use Ni centers bound to diaminodithiolate (S_2N_2) ligands.[4,6,15] Such tetradentate ligands probably constrain Ni to a square-planar geometry,[30] although square-pyramidal or octahedral NiS_2N_2 centers have been observed for Ni−Ru system where the fifth and sixth site are occupied by hydride and aquo ligands.[16] In the Ni-diphosphine catalysts, the coordination sphere at Ni is proposed to alternate between square-pyramidal (with a bridging hydride), tetrahedral, and, possibly, square planar geometries (Figure 11).

With respect to altering basicities and reduction potentials, this work revealed that terminal ligands on nickel are more influential than changes in the dithiolate. On the other hand, the nature of the dithiolate more strongly affects catalytic rates. The pK_a's of $[\mathbf{1}H]^+$ vs $[\mathbf{2}H]^+$ differ by 2 units in PhCN solution. The diphosphine dcpe is known to substantially enhance the basicity of its complexes relative to dppe. Angelici has shown that $Fe(CO)_3(dcpe)$ is more basic than $Fe(CO)_3(dppe)$ by about 4 $pK_a^{C_2H_4Cl_2}$ units.[31] Thus, it appears that the dcpe vs dppe effect is attenuated in the bimetallic system. In contrast, the change of $Fe(CO)_3$ to $Fe(PPh_3)(CO)_2$ leads to a $\Delta pK_a = 3-4$. The differing effect of substitution at Fe vs Ni suggests that the hydride is more strongly bonded to Fe.

An approximate thermodynamic analysis suggests that increasing the basicity of the diphosphine more strongly affects the redox properties of the NiFe complexes than their basicities. The $[NiFe(pdt)(dcpe)(CO)_3]^{0/+}$ couple is 250 mV more negative than the $[NiFe(pdt)(dppe)(CO)_3]^{0/+}$ couple in MePhCN solution (Table 2). A similar effect is seen for the dppe-edt and dcpe-edt complexes. The finding that the Ni-center more strongly affects the redox potential (6.88 kcal/mol at 298 K) than the basicity (2.6 kcal/mol at 298 K) suggests that oxidation of the Fe(I)Ni(I) complexes is localized at Ni, that is, corresponding to the couple Fe^INi^I/Fe^INi^{II}. Substitution of dppe for dcpe also causes the reduction of the hydrides to become more difficult by 200−250 mV. Therefore, compounds containing more basic diphosphines on Ni will necessarily have higher overpotentials for electrocatalytic reduction of protons. Trends in the basicities and redox potentials for the new NiFe complexes suggest that protonation occurs primarily at the Fe center, whereas reduction is shared over both Ni and Fe.

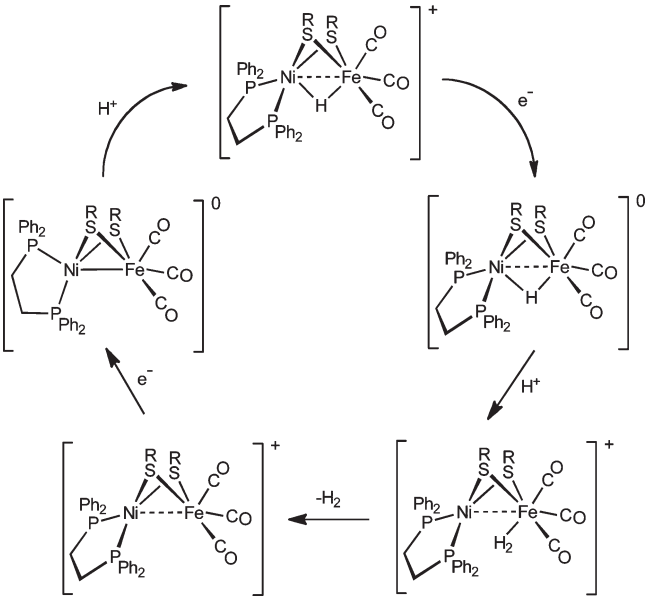

Figure 11. Proposed pathway for hydrogen evolution catalyzed by $NiFe(SR)_2$ complexes.

The new NiFe hydrides, like others of this type,[9] are active electrocatalysts for the production of hydrogen. The best catalysts operate at overpotentials of ∼500 mV at limiting rates near about 300 s^{-1}. Relative to the pdt derivatives, the edt-derived catalyst $[\mathbf{3}H]^+$ displays faster turnover rates, while maintaining the same overpotential. Complexes $[\mathbf{1}H]^+$ and $[\mathbf{3}H]^+$ exhibit very similar spectroscopic properties as well as similar reduction potentials and acidities. In the acid-independent regime, the differing rates of proton reduction thus must arise from intramolecular processes. As pointed out by Fraze et al.,[21] such intramolecular processes could include the coupling of two hydride ligands to form a bound dihydrogen or subsequent dissociation of H_2 from the metal. At 298 K, a 10x increase in rate requires a change in activation energy of 2.6 kcal.

The mechanism of hydrogen evolution by these Ni−Fe models begins with the reduction of the Fe(II)−Ni(II) hydride (Figure 11). In this respect, there exists close parallels between

dx.doi.org/10.1021/ic2012759 |Inorg. Chem. 2011, 50, 9554–9563

the catalytic cycles for the μ-hydrides of Ni−Fe dithiolates and Fe(II)−Fe(II) dithiolates.[32] Neither model system however follows the pathways likely for the biological catalysts: the [NiFe]-hydrogenases do not operate via Fe(I) intermediates[3,33] and the [FeFe]-hydrogenases do not operate via bridging hydrides.[34] It is however encouraging that the basic design inspired by biology is rather forgiving despite differences in geometry at Ni, terminal ligation at Fe and Ni, and the nature of the μ-thiolates. One possible reason for the high activity may be the stereochemical nonrigidity of the nickel sites in both NiFe(SR)$_2$(dxpe)(PR$_3$)$_x$(CO)$_{3-x}$ and the protonated derivatives [HNiFe(SR)$_2$(dxpe)(PR$_3$)$_x$(CO)$_{3-x}$]$^+$.

EXPERIMENTAL SECTION

Reactions were typically conducted using Schlenk techniques at room temperature. Most reagents were purchased from Aldrich and Strem, and unless otherwise stated, were used as received. Solvents were HPLC-grade and dried by filtration through activated alumina or distilled under nitrogen over an appropriate drying agent. Ni(pdt)(dppe),[35] Ni(SPh)$_2$(dppe),[36] Ni(SPh)$_2$(dmpe),[16] NiCl$_2$(dppbz),[37] NiCl$_2$(dcpe),[38] NiCl$_2$(dppf),[39] NiCl$_2$(dppp),[40] and **1**[12] were prepared according to modified literature procedures. Chromatography was conducted with Siliaflash P60 from Silicycle (230−400 mesh). HBF$_4$·Et$_2$O (Sigma-Aldrich) was supplied as 51−57% HBF$_4$ in Et$_2$O (6.91−7.71 M). A 2.0 M solution of HCl in Et$_2$O was purchased from Sigma-Aldrich. Bu$_4$NPF$_6$ was purchased from GFS Chemicals and was recrystallized multiple times by extraction into CH$_2$Cl$_2$ followed by precipitation by hexane. ^{1}H NMR spectra (500 or 400 MHz) are referenced to residual solvent relative to TMS. ^{31}P{^{1}H} NMR spectra (202 or 161 MHz) were referenced to external 85% H$_3$PO$_4$. FT-IR spectra were recorded on a Perkin-Elmer Spectrum 100 FT-IR spectrometer.

NiCl$_2$(dcpe). The published synthesis was followed,[38] but no NMR data had been reported. ^{31}P{^{1}H} NMR (CD$_2$Cl$_2$): δ 81.2(s). ^{1}H NMR (CD$_2$Cl$_2$): δ 1.2−2.6 (broad m).

Ni(pdt)(dcpe). A solution of 3.50 g (6.34 mmol) of NiCl$_2$(dcpe) in 30 mL of CH$_2$Cl$_2$ was treated with 0.685 g (6.34 mmol) of 1,3-propanedithiol followed by a solution of 1.37 g (25.3 mmol) of NaOMe in 10 mL of MeOH. The mixture was stirred for 15 min, during which time the color of the reaction solution deepened. Solvent was removed under reduced pressure, and the residue was extracted into CH$_2$Cl$_2$ (20 mL). The slurry was filtered through a pad of Celite to remove NaCl, and the dark orange filtrate was evaporated. Yield: 3.61 g (97%). ^{31}P{^{1}H} NMR (CD$_2$Cl$_2$): δ 72.3(s). Anal. Calcd for C$_{29}$H$_{54}$NiP$_2$S$_2$ (found): C 59.29 (59.57); H, 9.26 (9.33).

Ni(edt)(dcpe). A solution of 1.12 g (2.00 mmol) of NiCl$_2$(dcpe) in 20 mL of CH$_2$Cl$_2$ was treated with 0.188 g (2.00 mmol) of 1,2-ethanedithiol followed by 0.405 g (4.00 mmol) of triethylamine. The mixture was stirred for 30 min, during which time the color of the reaction solution deepened. Solvent was removed under reduced pressure, and the residue was washed with 3 × 10 mL portions of MeOH. The remaining orange solid was recrystallized by the addition of hexanes to a CH$_2$Cl$_2$ solution, and the resulting orange crystals were washed with 10 mL portions of hexanes and MeOH. Yield: 1.00 g (60%). ^{31}P{^{1}H} NMR (CD$_2$Cl$_2$): δ 78.4(s). Anal. Calcd for C$_{28}$H$_{52}$NiP$_2$S$_2$·CH$_2$Cl$_2$·2C$_6$H$_{14}$ (found): C 59.28 (59.58); H, 9.95 (9.24).

Ni(Me$_2$pdt)(dppe). A solution of NiCl$_2$(dppe) (2.65 g, 5.0 mmol) in 200 mL of CH$_2$Cl$_2$ was treated with 0.79 g (5.8 mmol) of Me$_2$pdtH$_2$, followed by 1.58 mL (11.6 mmol) of triethylamine causing the orange solution to become dark red. After stirring for 10 min, the solution was reduced to half volume, transferred to a separatory funnel, and extracted into an equal volume of water. The volume of the CH$_2$Cl$_2$ layer was reduced, diluted with hexanes, and stored at −20 °C, resulting in dark red crystals, which were washed with hexanes. Yield: 1.8 g (61%). ^{1}H NMR (CDCl$_3$): δ 7.84(d), 7.44 (m) (dppe C$_6$H$_5$), 2.25 (d) (S(CH$_2$)$_2$C), 2.14 (d) (P(CH$_2$)$_2$P), 0.96 (s) (C(CH$_3$)$_2$). ^{31}P{^{1}H} NMR (CDCl$_3$): δ 55.9(s).

[(I)NiFe(Me$_2$pdt)(dppe)(CO)$_3$]$^+$ and NiFe(Me$_2$pdt)I$_2$(dppe). In a 50 mL Schlenk flask were dissolved 0.140 g (0.24 mmol) of FeI$_2$(CO)$_4$ and 0.100 g (0.24 mmol) of Ni(Me$_2$pdt)(dppe) in 5 mL of CH$_2$Cl$_2$. After stirring the solution for 5 min, the IR spectrum of the mixture showed ν_{CO} = 2095, 2075, 2053, and 2020 cm^{-1}. To the red solution, 20 mL of hexanes was added to precipitate a red solid. The IR spectrum of the red solid contains ν_{CO} = 2095, 2053, and 2020 cm^{-1}, which is similar to that for the species formed by reaction of **1** with I$_2$. The red solid was extracted into 5 mL of CH$_2$Cl$_2$, and this solution was treated with 1 equiv of NaBF$_4$. After stirring for 1 h, the mixture was filtered through Celite, the filtrate was concentrated to 2 mL, and hexanes were layered over the solution. After storage at −20 °C, red and brown crystals had formed, which were identified as NiI$_2$(dppe) and NiFe(Me$_2$pdt)I$_2$(dppe), respectively, by X-ray diffraction.

[(CO)$_2$Fe(SPh)$_2$Ni(CO)]$_2$(μ-dppe)$_2$. A 100 mL Schlenk flask was charged 0.264 g (0.392 mmol) of Ni(SPh)$_2$(dppe)[41] and 0.142 g (0.390 mmol) of Fe$_2$(CO)$_9$ followed by 8 mL of tetrahydrofuran (THF). The mixture was stirred for 1 h. The solvent was removed under vacuum, and the residue was extracted into Et$_2$O. This extract was filtered through a pad of Celite and then evaporated under vacuum. After rinsing the residue with 2 × 10 mL of MeOH and 2 × 10 mL of hexane, a dark brown solid was obtained. Yield: 0.100 g (31%). IR (CH$_2$Cl$_2$): ν_{CO} 1993, 1938 cm^{-1}. ^{31}P{^{1}H} NMR (CD$_2$Cl$_2$): δ 33.9 (d), 49.9 (d). Single crystals were obtained from slow diffusion of hexane into a concentrated CH$_2$Cl$_2$ solution.

NiFe(pdt)(dcpe)(CO)$_3$ and [HNiFe(pdt)(dcpe)(CO)$_3$]BF$_4$, 2 and [2H]BF$_4$. A 100 mL Schlenk flask was charged 0.350 g (0.85 mmol) of FeI$_2$(CO)$_4$ and 0.500 g (0.85 mmol) of Ni(pdt)(dcpe). The flask was cooled to −78 °C. To the cooled mixture of solids was added 10 mL of CH$_2$Cl$_2$, resulting in a dark brown homogeneous solution. A 0.5 mL sample was removed (using an ambient temperature syringe) and checked by FT-IR spectroscopy to confirm the formation of the proposed μ-iodo intermediate (see Table 1). The remaining cold reaction solution was treated with 0.320 g (1.70 mmol) of Cp$_2$Co. The reaction solution became brown-green, and was allowed to warm to room temperature. After stirring for 1 h at room temperature, the reaction mixture was evaporated under reduced pressure, and the dark brown residue was washed and sonicated with 4 × 20 mL portions of MeCN (until the washings were colorless). The brown residue was extracted into 20 mL of CH$_2$Cl$_2$, and this solution of the product was filtered through a pad of Celite. The CH$_2$Cl$_2$ solution of the product was concentrated to dryness under vacuum. Yield: 0.4 g (62%). IR (CH$_2$Cl$_2$): ν_{CO} = 2015, 1941 cm^{-1}. ^{31}P{^{1}H} NMR (CD$_2$Cl$_2$): δ 81(s).

Into a solution of 0.150 g (0.207 mmol) of NiFe(pdt)(dcpe)(CO)$_3$ in 10 mL of CH$_2$Cl$_2$ was injected 100 μL (0.691 mmol) of HBF$_4$·Et$_2$O. An immediate color change from green-brown to dark orange was observed. The solution was concentrated under reduced pressure to about 5 mL, diluted with 30 mL of hexanes, and sonicated for 20 min to obtain a dark orange solid. The solid was filtered, and the reprecipitation method was repeated four cycles to afford a fine light orange powder. Yield: 0.09 g (53%). ^{31}P{^{1}H} NMR (CD$_2$Cl$_2$): δ 89.8(s). ^{1}H NMR (CD$_2$Cl$_2$): δ −3.00 (br. s, 1H, hydride). Anal. Calcd for C$_{32}$H$_{55}$BF$_4$FeNiO$_3$P$_2$S$_2$·CH$_2$Cl$_2$ (found): C, 44.03 (43.72); H, 6.38 (6.41). ESI-MS: m/z 727 ([M]$^+$). IR (CH$_2$Cl$_2$): ν_{CO} = 2078, 2017 cm^{-1}.

NiFe(pdt)(dppe)(CO)$_3$ and [(μ-I)NiFe(pdt)(dppe)(CO)$_3$]I. The procedure developed for NiFe(pdt)(dcpe)(CO)$_3$ was applied to the synthesis of **1**.[9] Yield: 0.22 g (38%). A solution of 30 mg (0.0426 mmol) of **1** in 5 mL of CH$_2$Cl$_2$ was cooled in a −78 °C bath and then treated with 10.8 mg (0.0426 mmol) of solid I$_2$. A 0.5 mL sample was removed and checked by FT-IR spectroscopy: ν_{CO} = 2095, 2055, 2025 cm^{-1} (see Figure 2).

dx.doi.org/10.1021/ic2012759 |Inorg. Chem. 2011, 50, 9554–9563

NiFe(edt)(dppe)(CO)$_3$ and [HNiFe(edt)(dppe)(CO)$_3$]BF$_4$, 3 and [3H]BF$_4$. A 100-mL Schlenk flask was charged with 0.382 g (0.91 mmol) of $FeI_2(CO)_4$ and 0.500 g (0.91 mmol) of Ni(edt)(dppe) and cooled to −78 °C. Thirty milliliters of CH_2Cl_2 was added to the cooled mixture, resulting in a dark brown homogeneous solution. A 0.5 mL sample was removed (using an ambient temperature syringe) and checked by FT-IR spectroscopy to confirm the formation of the proposed μ-iodo intermediate (see Table 1). The remaining cold reaction solution was then treated with a precooled (−78 °C) solution of 0.344 g (1.82 mmol) of Cp_2Co in 20 mL of CH_2Cl_2, which was transferred via cannula. The reaction solution became brown-green and was allowed to warm to room temperature. After stirring for 20 min at room temperature, the reaction mixture was evaporated under reduced pressure, and the dark green residue was washed with 2 × 30 mL of MeCN. The dark green residue was extracted into 20 mL of CH_2Cl_2, and the dark green product was precipitated by addition of 30 mL of hexanes. Yield: 0.42 g (71%). $^{31}P\{^1H\}$ NMR (CD_2Cl_2): δ 650 (s). IR (CH_2Cl_2): ν_{CO} 2029, 1957 cm^{-1}. The protonation was conducted analogously to the protonation of **1**. ^1H NMR (CD_2Cl_2): δ −5.7 (br s, 1H). $^{31}P\{^1H\}$ (CD_2Cl_2): δ 72.7. IR (CH_2Cl_2): ν_{CO} = 2084, 2025 cm^{-1}. Anal. Calcd for $C_{31}H_{29}BF_4FeNiO_3P_2S_2$ (found): C, 44.59 (44.40, 43.72); H, 3.63 (3.62, 3.5).

NiFe(edt)(dcpe)(CO)$_3$ and [HNiFe(edt)(dcpe)(CO)$_3$]BF$_4$, 4 and [4H]BF$_4$. A 100 mL Schlenk flask was charged with 0.62 g (1.46 mmol) of $FeI_2(CO)_4$ and 0.84 g (1.46 mmol) of Ni(edt)(dcpe). To the mixture was added 20 mL of CH_2Cl_2 at room temperature resulting in a brown solution. After stirring for 15 min at room temperature, the solution was treated with 0.55 g (2.92 mmol) of Cp_2Co, and was allowed to stir for 30 min. The reaction mixture was evaporated under reduced pressure, and the dark brown solid was washed with 4 × 15 mL portions of MeCN (until washings were clear). The crude product was filtered through a pad of silica gel with CH_2Cl_2 to remove unreacted starting Ni(edt)(dcpe). The CH_2Cl_2 solution was then concentrated to dryness under vacuum. The product could not be purified beyond removal of unreacted starting material.$^{31}P\{^1H\}$ NMR (CD_2Cl_2): δ 94.1(s). The protonation was conducted analogously to the protonation of **1**. ^1H NMR (CD_2Cl_2): δ −5.3 (br s, 1H). $^{31}P\{^1H\}$ (CD_2Cl_2): δ 92.0 (s). IR (CH_2Cl_2): ν_{CO} = 2080, 2019 cm^{-1}.

[HNiFe(edt)(dppe)(PPh$_3$)(CO)$_2$]BF$_4$ and NiFe(edt)(dppe)-(PPh$_3$)(CO)$_2$, 5 and [5H]BF$_4$. In a 250 mL round bottomed Schlenk flask, 0.760 g (0.98 mmol) of [HNiFe(edt)(dppe)(CO)$_3$]BF$_4$ was dissolved in 80 mL of THF. The solution was treated with 2.5 g (9.8 mmol) of PPh_3. After stirring the solution for 2 h at 40 °C, the solvent was removed in vacuum, yielding a red oil, which was washed with 3 × 40 mL portions of hexanes. The resulting reddish-brown powder was recrystallized by layering a CH_2Cl_2 solution with hexanes, which yielded orange crystals. Yield: 0.80 g (80%). ^1H NMR (CD_2Cl_2): −5.13 (dt), −8.15 (dt). $^{31}P\{^1H\}$ NMR (CD_2Cl_2): 71.5 (s, PPh_3 *unsym* or dppe *sym*), 67.1 (s, dppe *unsym*), 66.8 (s, PPh_3 *unsym* or dppe *sym*), 45.5 (s, PPh_3, *sym*). IR (CH_2Cl_2): ν_{CO} = 2019, 1968 cm^{-1}. Anal. Calcd for $C_{48}H_{44}BF_4FeNiO_2P_3S_2 \cdot CH_2Cl_2$ (found): C, 53.69 (53.34); H, 4.23 (4.48). IR (CH_2Cl_2): ν_{CO} = 2014, 1962 cm^{-1}.

A solution of 0.265 g (0.26 mmol) of [HNiFe(edt)(dppe)-(PPh$_3$)(CO)$_2$]BF$_4$ in 20 mL of CH_2Cl_2 and 5 mL of MeOH was treated with 0.014 g (0.26 mmol) of NaOMe in 10 mL of MeOH. The mixture stirred for 4 h, during which time the solution changed color from orange to green. Solvent was removed under vacuum, and the resulting green residue was washed with 3 × 15 mL portions of water and 3 × 10 mL portions of MeOH. $^{31}P\{^1H\}$ NMR (CD_2Cl_2, 20 °C): 74.9 (br, dppe), 54.7 (m, PPh_3), 48.4 (br, dppe). IR (CH_2Cl_2): ν_{CO} = 1968, 1912 cm^{-1}.

Electrochemistry. The nickel−iron hydrides presented in this paper degrade to uncharacterized products in MeCN solution ($t_{1/2} \sim 60$ min). For this reason, most electrochemical measurements were conducted in CH_2Cl_2 solutions. Cyclic voltammetry experiments were conducted using a 20 mL one-compartment glass cell with a tight-fitting Teflon top using a BAS-100 Electrochemical Analyzer. The working electrode was a glassy carbon (GC) disk (diameter = 3.00 mm). A silver wire was used as a quasireference electrode, and the counter electrode was a Pt wire. The electrolyte was 0.1 M $[Bu_4N]PF_6$. Ferrocene (sufficient to give ∼1 mM solution) was added as an internal reference, and each cyclic voltammogram was referenced to this $Fc^{0/+}$ couple = 0.00 V. *i*R compensation was applied to all measurements using the BAS software. Cell resistance was determined prior to each scan, and the correction was applied to the subsequently collected cyclic voltammagram. To account for catalysis by the GC electrode, control experiments were recorded at the same scan rate and potential range, and this current was subtracted as background. During prolonged experiments, additional solvent was added to compensate for evaporative loss. For measurements of i_p vs $[H^+]$, the total volume of acid solution (∼20 μL aliquots of 0.5 M acid) was less than 5% of the sample volume, and this effect was ignored. Between scans, the solution was purged briefly with N_2 and the working GC electrode was removed and polished. The duration of typical electrochemical titrations was 30 min.

Crystallography. *[HNiFe(pdt)(dcpe)(CO)$_3$]BF$_4$·CH$_2$Cl$_2$.* A structural model consisting of the host cation plus a disordered $[BF_4]^-$ anion and a dichloromethane solvate molecule was developed. All B−F and F---F distances in the disordered anion were restrained to be similar (0.01 and 0.02 esd's respectively). Rigid-bond restraints (esd 0.01) were imposed on displacement parameters for all disordered sites and similar displacement amplitudes (esd 0.01) were imposed on disordered sites overlapping by less than the sum of van der Waals radii. The metal hydride H atom was found in the difference map and was allowed to refine isotropically. The remaining H atoms were included as riding idealized contributors and their *U*'s were assigned as 1.2× carrier U_{eq}.

[HNiFe(edt)(dppe)(CO)$_3$]B$_2$OHF$_6$·CH$_2$Cl$_2$. A structural model consisting of the host ion pair plus one disordered dichloromethane solvate molecule was developed. Like bond distances and angles were restrained to be similar between the two orientations of the disordered dichloromethane solvate molecule (esd 0.01 and 0.02 respectively). Similar displacement amplitudes (esd 0.01) were imposed on disordered sites overlapping by less than the sum of van der Waals radii. Additionally, the displacement parameters were restrained to approximate to isotropic behavior for all disordered sites. The metal hydride was located in the difference map. The metal hydride distance was allowed to refine, but the H atom *U*'s were assigned as 1.5× U_{eq} of the carrier atom (The carrier atom was assumed to be Fe1 because the Fe−H distance was shorter than the Ni−H distance). The hydroxyl atom on the counterion[42] was located in the difference map. The O−H bond distance was allowed to refine, but the H atom *U*'s were assigned as 1.5× U_{eq} of the carrier O atom. The hydroxyl H atom was found to be hydrogen bonding to F5 on the counterion. Remaining H atoms were included as riding idealized contributors and their *U*'s were assigned as 1.2× carrier U_{eq}.

[(CO)$_2$Fe(SPh)$_2$Ni(CO)]$_2$(μ-dppe)$_2$. A structural model consisting of the molecule was developed. This model converged with w_{R2} = 0.0746 and R_1 = 0.0438 for 451 parameters against 8306 data. H atoms were included as riding idealized contributors. H atom *U*'s were assigned as 1.2× carrier U_{eq}.

NiFe(pdt)(dppe)I$_2$. A structural model consisting of the host plus 1/2 a disordered hexane solvate molecule per asymmetric unit was developed; however, positions for the idealized solvate molecules were poorly determined. This model converged with w_{R2} = 0.1387 and R_1 = 0.0514 for 366 parameters with 0 restraints against 6177 data. Since positions for the solvate molecules were poorly determined, a second structural model was refined with contributions from the solvate molecules removed from the diffraction data using the bypass procedure in PLATON.[43] No positions for the host network differed by more than two su's between these two refined models. The electron count

from the "squeeze" model converged in good agreement with the number of solvate molecules predicted by the complete refinement. The "squeeze" data are reported here. Methyl H atom positions, R-CH_3, were optimized by rotation about R-C bonds with idealized C−H, R--H, and H--H distances. Remaining H atoms were included as riding idealized contributors. Methyl H atom *U*'s were assigned as 1.5× U_{eq} of the carrier atom; remaining H atom *U*'s were assigned as 1.2× carrier U_{eq}.

■ ASSOCIATED CONTENT

Supporting Information. Crystallographic analyses and additional spectroscopic, electrochemical, and preparative details. This material is available free of charge via the Internet at http://pubs.acs.org.

■ AUTHOR INFORMATION

Corresponding Author
*E-mail: rauchfuz@illinois.edu.

■ ACKNOWLEDGMENT

This research was supported by the NIH. We thank David Schilter for helpful advice.

■ REFERENCES

(1) Cammack, R.; Frey, M.; Robson, R. *Hydrogen as a Fuel: Learning from Nature*; Taylor & Francis: London, U.K., 2001; Ogata, H.; Lubitz, W.; Higuchi, Y. *Dalton Trans.* **2009**, 7577–7587. Fontecilla-Camps, J. C.; Amara, P.; Cavazza, C.; Nicolet, Y.; Volbeda, A. *Nature* **2009**, *460*, 814–822. Fontecilla-Camps, J. C.; Volbeda, A.; Cavazza, C.; Nicolet, Y. *Chem. Rev.* **2007**, *107*, 4273–4303.

(2) Ohki, Y.; Tatsumi, K. *Eur. J. Inorg. Chem.* **2010**, *2011*, 973–985. He, T.; Tsvetkov, N. P.; Andino, J. G.; Gao, X.-F.; Fullmer, B. C.; Caulton, K. G. *J. Am. Chem. Soc.* **2010**, *132*, 910–911.

(3) Tard, C.; Pickett, C. J. *Chem. Rev.* **2009**, *109*, 2245–2274.

(4) Canaguier, S.; Artero, V.; Fontecave, M. *Dalton Trans.* **2008**, 315–325.

(5) Li, Z.; Ohki, Y.; Tatsumi, K. *J. Am. Chem. Soc.* **2005**, *127*, 8950–8951. Jiang, J.; Maruani, M.; Solaimanzadeh, J.; Lo, W.; Koch, S. A.; Millar, M. *Inorg. Chem.* **2009**, *48*, 6359.

(6) Perra, A.; Davies, E. S.; Hyde, J. R.; Wang, Q.; McMaster, J.; Schröder, M. *Chem. Commun.* **2006**, 1103–1105.

(7) Barton, B. E.; Whaley, C. M.; Rauchfuss, T. B.; Gray, D. L. *J. Am. Chem. Soc.* **2009**, *131*, 6942–6943.

(8) Barton, B. E. Ph.D. Thesis, University of Illinois at Urbana-Champaign, Urbana, IL, 2010.

(9) Barton, B. E.; Rauchfuss, T. B. *J. Am. Chem. Soc.* **2010**, *132*, 14877–14885.

(10) Lubitz, W.; Reijerse, E.; van Gastel, M. *Chem. Rev.* **2007**, *107*, 4331–4365.

(11) Zhu, W.; Marr, A. C.; Wang, Q.; Neese, F.; Spencer, D. J. E.; Blake, A. J.; Cooke, P. A.; Wilson, C.; Schröder, M. *Proc. Natl. Acad. Sci.* **2005**, *102*, 18280–18285.

(12) Lever, A. B. P. *Inorg. Chem.* **1990**, *29*, 1271–1285.

(13) Whaley, C. M. Ph.D. Thesis, University of Illinois at Urbana-Champaign, Urbana, IL, 2009.

(14) Rakowski DuBois, M.; DuBois, D. L. *Acc. Chem. Res.* **2009**, *42*, 1974–1982.

(15) Canaguier, S.; Field, M.; Oudart, Y.; Pécaut, J.; Fontecave, M.; Artero, V. *Chem. Commun.* **2010**, *46*, 5876–5878 For work on related Ru-Ni systems, see Vaccaro, L.; Artero, V.; Canaguier, S.; Fontecave, M.; Field, M. J. *Dalton Trans.* **2010**, *39*, 3043–3049.

(16) Ogo, S. *Chem. Commun.* **2009**, 3317–3325.

(17) Ichikawa, K.; Matsumoto, T.; Ogo, S. *Dalton Trans.* **2009**, 4304–4309.

(18) Angamuthu, R.; Bouwman, E. *Phys. Chem. Chem. Phys.* **2009**, *11*, 5578–5583.

(19) Singleton, M. L.; Jenkins, R. M.; Klemashevich, C. L.; Darensbourg, M. Y. *C. R. Chim.* **2008**, *11*, 861–874.

(20) Bierbach, U.; Saak, W.; Haase, D.; Pohl, S. *Z. Naturforsch.* **1990**, *B45* (1990), 1945–1945.

(21) Fraze, K.; Wilson, A. D.; Appel, A. M.; Rakowski DuBois, M.; DuBois, D. L. *Organometallics* **2007**, *26*, 3918–3924.

(22) Izutsu, K. *Acid-Base Dissociation Constants in Dipolar Aprotic Solvents*; Blackwell Scientific Publications: Oxford, U.K., 1990.

(23) Felton, G. A. N.; Glass, R. S.; Lichtenberger, D. L.; Evans, D. H. *Inorg. Chem.* **2006**, *45*, 9181–9184. Fourmond, V.; Jacques, P.-A.; Fontecave, M.; Artero, V. *Inorg. Chem.* **2010**, *49*, 10338–10347. See also Koper, M. T. M.; Bouwman, E. *Angew. Chem., Int. Ed.* **2010**, *49*, 3723–3725.

(24) Kilgore, U. J.; Roberts, J. A. S.; Pool, D. H.; Appel, A. M.; Stewart, M. P.; Rakowski DuBois, M.; Dougherty, W. G.; Kassel, W. S.; Bullock, R. M.; DuBois, D. L. *J. Am. Chem. Soc.* **2011**, *133*, 5861–5872.

(25) Kaljurand, I.; Kütt, A.; Sooväli, L.; Rodima, T.; Mäemets, V.; Leito, I.; Koppel, I. A. *J. Org. Chem.* **2005**, *70*, 1019–1028.

(26) Hieber, W.; Bader, G. *Ber. Deutsch. Chem. Ges.* **1928**, *61B*, 1717–1722. Manuel, T. A. *Inorg. Chem.* **1963**, *2*, 854–858. Cohen, I. A.; Basolo, F. *J. Inorg. Nucl. Chem.* **1966**, *28*, 511–520. Li, B.; Liu, T.; Popescu, C. V.; Bilko, A.; Darensbourg, M. Y. *Inorg. Chem.* **2009**, *48*, 11283–11289. Moreland, A. C.; Rauchfuss, T. B. *Inorg. Chem.* **2000**, *39*, 3029–3036. Verhagen, J. A. W.; Lutz, M.; Spek, A. L.; Bouwman, E. *Eur. J. Inorg. Chem.* **2003**, *2003*, 3968–3974. Jiang, J.; Koch, S. A. *Inorg. Chem.* **2002**, *41*, 158–160. Turrell, P. J.; Wright, J. A.; Peck, J. N. T.; Oganesyan, V. S.; Pickett, C. J. *Angew. Chem., Int. Ed.* **2010**, *49*, 7508–7511.

(27) Bellachioma, G.; Cardaci, G.; Macchioni, A.; Venturi, C.; Zuccaccia, C. *J. Organomet. Chem.* **2006**, *691*, 3881–3888. Jiang, J.; Lo, W.; Müller, P.; Fine, N. D.; Maruani, M.; Raytman, A. *Inorg. Chem. Commun.* **2009**, *12*, 527–529.

(28) Benito-Garagorri, D.; Lagoja, I.; Veiros, L. F.; Kirchner, K. A. *Dalton Trans.* **2011**, *40*, 4778–4792.

(29) Duan, L.; Wang, M.; Li, P.; Wang, N.; Wang, F.; Sun, L. *Inorg. Chim. Acta* **2009**, *362*, 372–376.

(30) Grapperhaus, C. A.; Darensbourg, M. Y. *Acc. Chem. Res.* **1998**, *31*, 451–459.

(31) Sowa, J. R., Jr.; Zanotti, V.; Facchin, G.; Angelici, R. J. *J. Am. Chem. Soc.* **1992**, *114*, 160–165.

(32) Ezzaher, S.; Capon, J.-F.; Dumontet, N.; Gloaguen, F.; Pétillon, F. Y.; Schollhammer, P.; Talarmin, J. *J. Electroanal. Chem.* **2009**, *626*, 161–170.

(33) Wu, H.; Hall, M. B. *C. R. Chim.* **2008**, *11*, 790–804. Siegbahn, P. E. M.; Tye, J. W.; Hall, M. B. *Chem. Rev.* **2007**, *107*, 4414–4435.

(34) Gloaguen, F.; Rauchfuss, T. B. *Chem. Soc. Rev.* **2009**, *38*, 100–108.

(35) Schmidt, M.; Hoffmann, G. G. *J. Organomet. Chem.* **1977**, *124*, C5–C8.

(36) Hayter, R. G.; Humiec, F. S. *J. Inorg. Nucl. Chem.* **1964**, *26*, 807–810.

(37) Levason, W.; McAuliffe, C. A. *Inorg. Chim. Acta* **1974**, *11*, 33–40.

(38) Angulo, I. M.; Bouwman, E.; van Gorkum, R.; Lok, S. M.; Lutz, M.; Spek, A. L. *J. Mol. Catal. A* **2003**, *202*, 97–106.

(39) Corain, B.; Longato, B.; Favero, G.; Ajò, D.; Pilloni, G.; Russo, U.; Kreiss, F. R. *Inorg. Chim. Acta* **1989**, *157*, 259–266.

(40) Bomfim, J. A. S.; de Souza, F. P.; Filgueiras, C. A. L.; de Sousa, A. G.; Gambardella, M. T. P. *Polyhedron* **2003**, *22*, 1567–1573. Van Hecke, G. R.; Horrocks, W. D., Jr. *Inorg. Chem.* **1966**, *5*, 1968–1974.

(41) Rauchfuss, T. B.; Shu, J. S.; Roundhill, D. M. *Inorg. Chem.* **1976**, *15*, 2096–2101.

(42) Kuhn, N.; Göhner, M.; Steimann, M. *Z. Anorg. Allg. Chem.* **2003**, *629*, 595–596.

(43) Spek, A. L.; van der Sluis, P. *Acta Crystallogr.* **1990**, *A46*, 194–201.

■ NOTE ADDED AFTER ASAP PUBLICATION

This paper was published on the Web on August 25, 2011, with the incorrect artwork for the TOC and Abstract graphics. The corrected version was reposted on August 29, 2011.